Author Response to Reviewer comments

Major issues

> ** page 2, line 21: The authors use a fixed value for the solar wind velocity. I think it would be very beneficial to use solar wind measurements from OMNI to determine the aberration angle specifically for each magnetopause crossing. A fixed aberration angle results in an additional source of variation in the observed magnetopause location (in the aberrated/model system); it may well account for that variation being larger than what is predicted by model errors (e.g. Figure 4).*

We changed to use individual solar wind conditions to calculate the aberration angle for each crossing. To achieve this, OMNI measurements are propagated from the Bow Shock Nose to the MP location (on the x-axis).

> ** page 3, line 8 and Figure 1: Shue et al. specifically use the innermost crossings of the magnetopause. To validate their magnetopause model, the authors of this manuscript should use the same methodology. Otherwise the results will not necessarily be quantitatively comparable. The choice of the outermost crossings may be the reason for the "tendency of the magnetopause to be found at greater distance to the magnetotail than expected" (caption of Figure 4). Furthermore, Figure 1 seems to reveal that the authors do actually use the innermost magnetopause crossings, contrary to what is stated in the text. A zoom-in to the interval between 6 - 7 UT shows that THC crossed the magnetopause multiple times. I would identify the last (outermost) crossing at about 06:47:30 UT. The crossing at 06:14 UT indicated in the figure caption would be the innermost crossing, in my opinion.*

All crossings were revaluated to get a complete list of all crossings, not just the outermost. This enabled us to choose the same methodology as Shue et al. and complement our analysis by choosing the innermost and outermost crossing respectively. We thank the author for this very helpful observation, because the accuracy of the investigation could be improved significantly.

> ** page 3, line 12: "projected onto the xy_GSM-plane": This is not good, because the projection is not only used for illustrative purposes, but also to ascertain the accuracy of the model at lunar distances. The model is axis-symmetric around the x-axis of an aberrated GSE/GSM coordinate system. Hence, sqrt(yˆ2 + zˆ2) should be used as axis perpendicular to x for comparison with the model, and not a projection onto (aberrated) GSM xy. This issue affects all Figures and sections from 2.3 onwards, e.g.: usage of Delta y in section 3 and projections onto xy in section 4.*

For better visualization we changed to the proposed representation.

> ** page 4, line 17/18: A lack of correlation between normalized Delta y and x does not necessarily mean that there is no systematic deviation between model and actual magnetopause. It just means that the spread in Delta y is very large. If the model were perfect and the magnetopause not as dynamic as it is, we would expect Delta y to be zero over the entire range of x values. Hence, there would be a very high correlation.*

Unfortunately, we are not sure what is meant by this comment. Maybe it would be possible to clarify? From our point of view, the lack of correlation shows that the normalized error of MP distance does not have any systematic dependence on the named variables.

> ** page 9, lines 5 to 10: There are a number of issues with the conclusions stated in this paragraph. The "tendency to agglomerate around the predicted directions" suggests that the flaring given by the model function is correct within the (very large) uncertainty limits of the angles determined by MVA (see large alpha and beta axis ranges in Figures 8 and 9). But this is to be expected should the model predict the magnetopause location accurately from the subsolar region to about 30 Earth radii downtail, as shown in Shue et al. (1997), and further on at 50-60 Earth radii downtail, as shown in this paper. Hence, in my opinion, the angular information inferred from the MVA is practically useless when evaluating the accuracy of the magnetopause model (including the assumption of axial symmetry). Again, the reason is the large scatter in the angles alpha and beta. The authors state that this scatter comes from the variability of the magnetopause position caused by constantly changing solar wind conditions, which I think is incorrect. Changing solar wind conditions should lead to a change in the magnetopause location, but not to a large change in normal directions. With MVA, the authors obtain estimates of instantaneous local normal directions, which will many times be very different to the reference or average normal direction even under constant solar wind conditions, due to the presence of surface waves or vortices (e.g., KHI).*

We hope the corresponding paragraph is now more clear, information on KHI is added.

“which will many times be very different to the reference or average normal”: We think with looking to the angle distribution this problem is addressed. What we get is just an average situation from the angle distribution, which then agrees to the model deduced normal direction.

Maybe you could clarify your remark?

Minor issues and technical corrections

> ** page 1, line 2: "10 Earth radii": The way this sentence is written is confusing, because the magnetopause is usually more than 10 Earth radii away from the Earth’s center, even in the subsolar region. The expression "10 Earth radii" probably refers only to the X-component of the locations.*

Clarified that the x-axis is meant here.

> ** page 1, line 3: "direction": At this point of the manuscript it is unclear that the authors refer to the direction normal to the magnetopause surface.*

“normal direction” is added.

> ** page 1, line 6: "reasonably": This could be quantified or described more accurately in the abstract.*

Removed in the new version.

> ** page 1, line 9: "is defined": Pressure balance is a feature of the equilibrium magnetopause, not necesarily the definition of the boundary.*

The definition of Baumjohan & Treuman, 1996, is added which defines the MP as the region between planetary magnetic field and solar wind plasma.

> ** page 1, line 11: "very advanced": What does "very advanced" exactly mean here? I would rather say that the main virtue of the model is its simplicity.*

Changed to “simple” which is a more accurate description.

> ** page 1, line 11: "normal direction": Actually, the model only predicts the distance of the magnetopause as a function of angle to the Earth-Sun-line. Based on this function, reference/average normal directions may be determined for every point on the model magnetopause surface.*

We added that the normal direction is only deduced from the model but is not originally predicted by it.

> ** page 1, line 15: "found this form to be only depended": They only made it dependend on Bz and Dp, but did not necessarily test dependences on other solar wind parameters.*

Clarified that the model was designed in that way and not the result of an broader analysis.

> ** page 1, line 16/17: "axially symmetric around the x-axis in GSE and GSM": This is not correct. The model is valid in aberrated GSE or GSM coordinate systems, where the solar wind approaches Earth exactly along the x-axis (see beginning of section 2.2).*

Aberration correction is added.

> ** page 2, line 22: "unless otherwise indicated": Are there any indications? I have not found any.*

The subclause was removed.

> ** page 2, line 25: "five minutes before and after": How is this choice motivated? Would a different choice of intervals lead to better MVA eigenvalue ratios?*
>
> ** page 2, line 31: "MP": Do the authors mean "spacecraft" here?*

The MP is actually meant here, since the positions of the MP and the spacecraft coincide during the crossing.

> ** page 3, line 2: The first sentence of section 2.3 sounds strange, because of the inserted subclause. Please reword.*

Sentence reworded: “Time periods of possible MP crossings are manually selected from the available ESA and FGM data sets when the spacecraft is located near the MP position as predicted by the Shue model. Here, “near” means about ± 10 R_E on the xy-plane around the predicted position.”

> ** page 3, line 6: "changes crossing": Sounds strange.*

Reworded to “changes when crossing”.

> ** page 3, line 14: "gather around their expected position": This sentence sounds somewhat strange to me. In addition, I don’t think that this can be seen in the figure, as each magnetopause crossing will take place under somewhat different*

solar wind conditions. Hence, the model magnetopause will look different each time. Figure 2, instead, only shows one model magnetopause for average conditions.

This is correct and the sentence is removed as well as the average Shue-MP from the Figure.

** page 4, first paragraph of section 3: The whole paragraph is written in a very confusing way. Please define and explain clearly in the text what is meant by: MP model range (use equations from Shue et al. if necessary), MP distance (I guess distance between the location of an ARTEMIS spacecraft at the time it was crossing the magnetopause to the predicted model magnetopause along y), delta y, determined MP (I guess "location" is missing here), delta r / 2 (this is not even defined in Figure 3), and parallax errors (I am not sure this term is really applicable here, see also page 6 line 13).*

The paragraph is rewritten in a hopefully more concise way.

** page 4, line 14: "very similar statistical properties": What does this mean? Please explain in more detail.*

With the new analysis this was removed.

** page 4, line 16: Should be "coefficients".*

With the new analysis this was removed.

** Figures 4 and 5: Define clearly "normalized error of MP distance" (used in both Figures 4 and 5), "relative MP position" as well as "normalized MP distance" in the captions. Why are three different terms used here?*

Also reworded and hopefully defined more concise.

** caption of Figure 5: "position of the MP projected": It is not possible to project the magnetopause surface onto a single point on the x axis. Please reword carefully.*

The location of the MP crossing was meant and the sentence was reworded.

** page 6, last paragraph: Use "°" instead of "degrees". Line 18: degrees is misspelled.*

Changed in the proposed way.

** page 6, last line: "one crossing per spacecraft and month": What is the reason for this restriction?*

This is due to the spacecraft orbit. We added that information.

** page 7, second to last line: "the observed scattering is not surprising": I do not understand this. Even if there were more crossings in the data set, the scattering would not be any lower, I suppose. Please explain.*

Unfortunately, we are not completely sure what was the problem with that.

** page 9, lines 12/13: "most adequately" and "most important drivers": In reference to what? I am not sure the results of this study allow for any conclusion on the relative importance of Bz and Dp with respect to other parameters.*

Due to the new analysis this part was removed.

Overall, we would like to thank the reviewer for the good and helpful comments, which hopefully helped to improve our analysis.

Statistical Analysis of Magnetopause Crossings at Lunar Distances

Johannes Z. D. Mieth[1], Dennis Frühauff[1], and Karl-Heinz Glassmeier[1]

[1]Technische Universität Braunschweig, Institut für Geophysik und extraterrestrische Physik, Mendelsohnstraße 3, 38106 Braunschweig, Germany

Correspondence: Johannes Z. D. Mieth (j.mieth@tu-braunschweig.de)

Abstract. Different magnetopause models with a diverse level of complexity are in use. They have in common to be mainly based on near-earth observations, i.e., they use measurements at distances of about ± 10 Earth radii along the GSM x-axis. Only very few observations of magnetopause crossings at larger distances are used for model fitting. In this study we compare position and normal direction predictions of the Shue et al. (1997) magnetopause model with actual observations of magnetopause crossings identified using the ARTEMIS spacecraft at lunar distance, about 60 Earth radii. We find ~~very good agreement between prediction and observation for the magnetopause position. Also the magnetopause normal directions are reasonably well predicted~~differences in the location prediction between model and actual observation but good agreement in predictions about the magnetopause normal direction.

1 Introduction

The magnetopause plays an important role for space weather processes as it is the primary interaction zone between the solar wind plasma and the Earth's magnetosphere. The magnetopause is defined as the boundary between solar wind and magnetospheric plasma which can not be penetrated by the solar wind (Baumjohann and Treumann, 1996). In case of an equilibrium magnetopause this is the plane where the solar wind pressure is balanced by the Earth's magnetic field pressure (e.g. Glassmeier et al., 2008). In 1997 Shue and co-workers presented a very ~~advanced~~ simple model to predict the magnetopause (MP) position ~~and its normal direction~~ under different solar wind (SW) conditions (Shue et al., 1997). Additionally to the location prediction it is possible to also deduce the MP normal direction. Using data of magnetopause crossings of the ISEE 1 and 2, AMPTE/IRM, and IMP 8 satellites they modelled the magnetopause radial distance r with the functional form $r = r_0 \left[2/\left(1+\cos\theta\right)\right]^{\alpha}$. Here r_0, θ, and α denote the standoff distance, the angle between the Sun-Earth line and the direction of r, and the magnetopause flaring parameter, respectively (Fig.3). Shue et al. (1997) ~~found this form~~ modelled the MP location to be only depended on the B_z component of the interplanetary magnetic field (IMF) and the solar wind dynamic pressure D_p. This functional model is mathematical axially symmetric around the x-axis in solar wind aberration corrected geocentric solar ecliptic (GSE) and geocentric solar magnetospheric (GSM) coordinates (Hapgood, 1992). Measurements used for the determination of the fitting parameters are mainly from distances of ± 10 Earth radii (R_E) on the x-axis with only a few data points expanding up to about $30\,\mathrm{R_E}$ downtail. As ~~detailed~~ precise the Shue model is, it requires further observations from higher latitudes as well as crossings further downtail from the Earth to provide a more realistic 3D magnetopause model (Shue and Song, 2002). Extensions of the Shue model were thus presented by, e.g., Lin et al. (2010) and Wang et al. (2013). However,

all the proposed models are still characterized by using only a very limited number of measurements at greater distances downtail. This is where our study contributes. By using plasma and magnetic field measurements from the ARTEMIS mission we validate the Shue model at radial distances of about $60\,\mathrm{R_E}$ downtail.

2 Data selection and analysis procedure

The *Acceleration, Reconnection, Turbulence, and Electrodynamics of the Moon's Interaction with the Sun* (ARTEMIS) Mission (Angelopoulos, 2010) provides long term measurements of the plasma environment in the terrestrial magnetosphere at lunar distances, about $60\,\mathrm{R_E}$. Since 2011 the two spacecraft THB and THC orbit the Moon and provide excellent measurements of the plasma environment there. The THB and THC spacecraft originate from the THEMIS mission (Angelopoulos, 2008), a NASA Medium-Class Explorers (MIDEX) mission, launched on February 17, 2007 and designed to investigate the trigger mechanisms and evolution of magnetospheric substorms. Five identical spacecraft were put into Earth's orbit to line up along the magnetotail. After the primary mission phase the two outermost spacecraft were lifted into a lunar orbit. Since May 2011 both probes are in stable equatorial and eccentrical orbits.

2.1 Observations

Our study covers a time span of five years, starting January 2011 and lasting until December 2015. Different types of data products are used to determine magnetopause position and direction. The electrostatic analyzer (ESA) (McFadden et al., 2008) provides ion and electron flux density over a broad energy band from only a few eV up to $30\,\mathrm{keV}$. We use time resolved ion energy data with a resolution of about $3\,\mathrm{s}$ in this study. In order to generate this data set, measurements with higher temporal resolution are integrated over a spin period of the spacecraft. The plasma data are complemented by measurements from the ARTEMIS fluxgate magnetometer (FGM) (Auster et al., 2008), providing vector magnetic field data which we average over the spin period of about 3 s.

2.2 Data processing

~~The spacecraft position vector~~

Since the MP behaviour depends on the instantaneous properties of the solar wind, measurements of the same are required. Such measurements are provided by NASA/GSFC's OMNI data set through OMNIWeb of which we extracted 1-minute solar wind magnetic field and plasma data for the desired time range. The magnetic field information as well as the ~~measured magnetic field vector are first represented in the~~ solar wind velocity is provided in an aberration corrected GSE coordinate system~~and corrected by a mean solar wind aberrationangle $\alpha = \tan^{-1}(v_\mathrm{E}/v_\mathrm{SW})$, with $v_\mathrm{E} = 30\,\mathrm{kms}^{-1}$, the velocity of~~ . Contrary, the extracted position information for a MP crossing underlies SW aberration. To calculate the individual aberration angle for each crossing, the ~~Earth around the Sun and $v_\mathrm{SW} = 400\,\mathrm{kms}^{-1}$, a commonly used value for the mean solar wind speed (Hansen et al., 2007). The aberration corrected data are~~ SW velocity $v_\mathrm{SW}(t_0)$ within a time range of a few hours before the crossing is extracted from OMNI. From this the time $t_\mathrm{SW}(v_\mathrm{SW}(t_0))$ can be calculated which the solar wind needs to propagate

from the Bow Shock Nose (BSN) to the MP position along the x-axis . The actual SW properties can then be extracted when the condition

$$\min\left(\left|t_{\mathrm{SW}}\left(v_{\mathrm{SW}}\left(t_0\right)\right)-t_0\right|\right) \tag{1}$$

is fulfilled. Afterwards position data and magnetic field data of each crossing can be corrected by the aberration angle and subsequently transformed into GSM coordinates. ~~Unless otherwise indicated GSM coordinates are always aberration corrected in the following.~~ However, as OMNI data is prepared for the situation before the BSN, the transitional conditions at the BSN have to be taken into account. To do so, Rankine-Hugoniot conditions are applied to the SW velocity by multiplying with a factor of $1/4$. OMNI SW data is also taken as the input parameter for the Shue model.

To determine the MP normal direction, minimum variance analysis (MVA) (e.g., Paschmann and Daly, 1998) is applied to the magnetic field data within five minutes before and after any identified MP crossing, which will be defined below. As the MVA analysis only provides the orientation but not the direction of the normal, we assume the magnetopause normal to be always directed outwards of the MP, into the direction of the magnetosheath.

~~To calculate model predictions of MP positions, SW observations are needed as input parameters to the Shue model. We use 1-minute solar wind magnetic field and plasma data as extracted from NASA/GSFC's OMNI data set through OMNIWeb. This dataset contains information on the plasma parameters at the bowshock's nose. To take into account the time delay between bowshock's nose observations and conditions at the actual MP position 1-hour mean averages of solar wind parameters are used to determine the model values of the MP position and normal direction.~~

2.3 Identifying MP crossings

Time periods of possible MP crossings are manually selected from the available ESA and FGM data sets when the spacecraft is ~~near, which means about $\pm 10\,\mathrm{R_E}$,~~ located near the MP position as predicted by the Shue model. Here, "near" means about $\pm 10\,\mathrm{R_E}$ on the xy-plane around the predicted position. The actual crossings are subsequently identified by visual inspection of ESA and FGM measurements. The magnetosheath plasma is characterized by a significant energy flux around $1\,\mathrm{keV}$. This flux almost instantly ceases once the MP has been crossed (Paschmann et al., 1993), see Fig. 1. Furthermore, also the particle number density, as derived from the energy spectrum, exhibits discontinuous changes ~~crossing at~~ when crossing the MP. In this way the precise crossing times and conditions are determined. Usually multiple crossings of the MP are also detected during the spacecraft motions into and out of the magnetotail. ~~Contrary to Shue et al. (1997) the outermost~~ Like in Shue et al. (1997) the innermost crossing is selected for further analysis in the current study. ~~As the outermost crossing~~ In order to extend the analysis further, the outermost crossing is also considered separately. As the innermost crossing we denote the ~~first (last~~ last (first) MP crossing of an ~~inbound (outbound~~ outbound (inbound) pass through the boundary region. In the case of the outermost, it is exactly the opposite.

A total of ~~244~~ 227 transitions is found ~~in this way. For 237~~ this way, innermost and outermost crossings respectively. For 225 of these SW data ~~are~~ is available. Figure 2 displays the spatial distribution of the MP positions determined ~~, projected onto the xy_{GSM}~~ on an xd-plane. ~~The figure also shows the expected mean model MP which is acquired by averaging solar wind~~

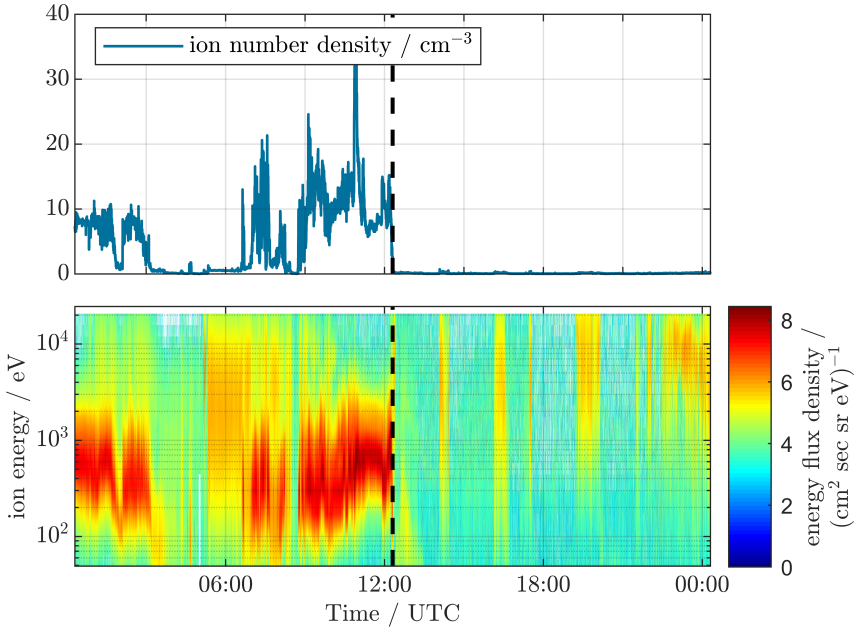

Figure 1. Example for MP crossing of ~~THC~~ THB on ~~27 February~~ 24 April 2013. The probe comes from the magnetosphere and enters the magnetosheath at around ~~0614~~ 1218 UTC.

~~dynamic pressure and the IMF B_z of all crossing events and using these as~~ X is the GSM/GSE axis, whereas $d = \pm\sqrt{y^2 + z^2}$. The sign is equal to the sign of the ~~model input parameters. One can easily see that all found MP positions nicely gather around their expected position.~~ y-component so that in- and outbound can be distinguished and either position can be visualized better. Using d as a measure for the distance of the MP crossing from the x-axis supports the view of the model as axial symmetric and removes any projection errors in case of a projection onto any of the GSM planes. Shown as a red dot are the mean positions of each independent point clouds~~which fall almost exactly onto the model MP~~.

3 Comparison of position predictions

Figure 3 shows all necessary variables of the the Shue model and our convention to compare actual positions with it. As the Shue model fits empirical data, fitting parameters a_1 to a_7 for the standoff distance r_0 and the flaring parameter α come with uncertainties (Shue et al., 1997).

$$r_0 = \begin{cases} (a_1 + a_2 B_z)(D_p)^{-\frac{1}{a_4}}, & \text{for } B_z \geq 0 \\ (a_1 + a_3 B_z)(D_p)^{-\frac{1}{a_4}}, & \text{for } B_z < 0 \end{cases} \tag{2}$$

$$\alpha = (a_5 + a_6 B_z)(1 + a_7 D_p) \tag{3}$$

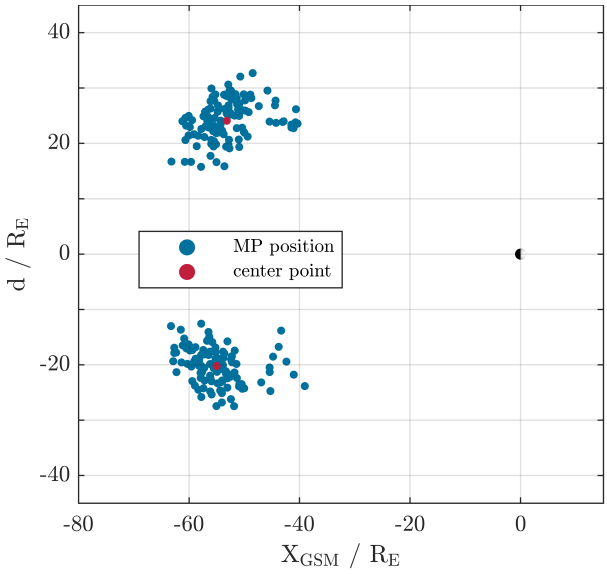

Figure 2. Distribution of MPs ~~projected onto xy_{GSM}~~displayed on $x_{GSM}d$-plane~~. The dashed line shows the mean model magnetopause, for which SW dynamic pressure and magnetic field B_z-component are averaged~~with $d = \pm\sqrt{y^2 + z^2}$, see text. The centre points of each independent point cloud is indicated by the red dots.

Equations 2 and 3 are equations 10 and 11 in Shue et al. (1997).

We interpret this uncertainty as a measure of the standard deviation of the predicted MP position. ~~The resulting MP model range is indicated by the dashed lines in Fig. 3.~~ If any MP ~~distance~~ position derived from ARTEMIS observations ~~fall into the thus defined error range δy, see Fig. 3,~~ falls into this standard deviation, we regard this MP ~~distance~~ position as compatible with the model. ~~We now define the distance between the modelled mean and minimum (maximum)MP distance along the~~ This leads to a minimum and maximum modelled MP location, depending if the minimal or maximal error is added to the fitting parameters. These are shown as dashed lines in Fig. 3. Using the best fit parameters without any fitting errors lead to the mean MP location (solid line).

As the MP is almost parallel to the x-axis at lunar distances, we concentrate on differences between position prediction and actual position along the previously described d-axis, or, as we rotated all positions into the equatorial (xy-)plane, along the y-axis. Rotating into the equatorial plane or using the defined d-axis ~~as the prediction error $\delta y/2$. In a subsequent step the difference Δy between the predicted and actually determined MP,~~ is equal to each other.

The standard deviation, which is the distance between minimum and maximum location along the y-axis, is ~~normalized to the prediction error $\delta r/2$.Since the magnetopause is almost aligned with the x-axis at lunar distances, no parallax errors need to be taken into account.~~ called error range δy by us, see Fig. 3. To quantify the actual MP position in relation to the model, its distance Δy to the mean model location is normalized to $\delta y/2$. We call this the normalized error of MP distance. Using this

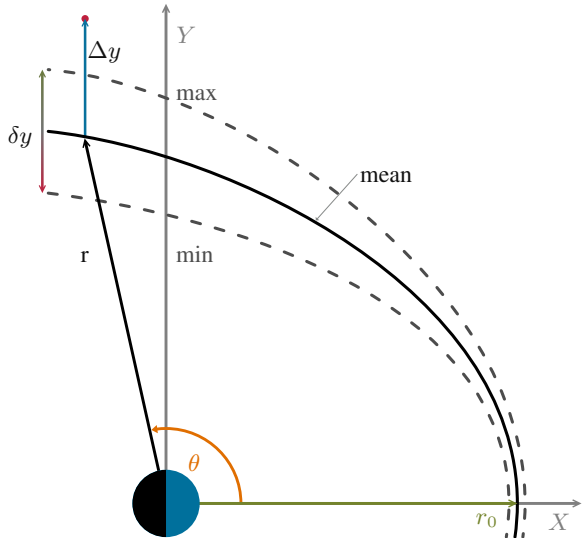

Figure 3. Scheme of the Shue et al. model and the normalization we ~~used~~use. The crossing of the MP with the x-axis is the standoff distance r_0. At certain angle θ the radial distance r of the MP is given. Fitting uncertainties by the model are indicated by the dashed lines. Not shown is the flaring effect α. To characterize the MP position (red dot) the difference distance along the y-axis between model and data, Δy, is normalized by half the error range, δy. (Graphic is not to scale.)

definition a MP laying exactly at the position predicted by the model has a ~~distance Δy~~ normalized distance $2\Delta y/\delta y$ of zero. A MP laying exactly at the model MP with error has the ~~distance Δy~~ normalized distance $2\Delta y/\delta y$ of ± 1.

Figure ~~??~~ 4 shows the distribution of normalized positions ~~. Approximately 53% of the MPs are within the model error as indicated by the vertical dashed dotted red lines. The mean is at $+0.18$~~ for the innermost crossing and Fig. 5 for the outermost crossing. In case of the innermost crossing the mean distance is at -1.12 with a standard deviation of ~~1.56. About 72.2% of the data lie within the 1σ-interval and 94.5% within the 2σ-interval. The distribution mostly follows a normal distribution and has very similar statistical properties to the Shue~~ 1.94 and a skewness of 0.76. This means that the MP is usually found more close to the magnetotail as predicted by the model. In about 54% of the crossings the model overestimates the location of the MP.

The situation is different with an outermost crossing, see Fig. 5. Here the mean distance is 2.48 with a standard deviation of 2.37 and a skewness of 0.89. Accordingly the location of the MP is underestimated by the model.

The normalized MP distance does not show any strong correlation to the MP position along the x_{GSM}-axis, the strength of the SW B_z-component, or the SW speed. Each of the respective correlation coefficient is below ~~0.4~~0.6. As an example, ~~Figure ?? displays~~ Figures 6 and 7 display the scattering of the x-position against the normalized distance. Because of that, we conclude that there is no systematic deviation between modelled and actually observed MP distance with respect to these parameters.

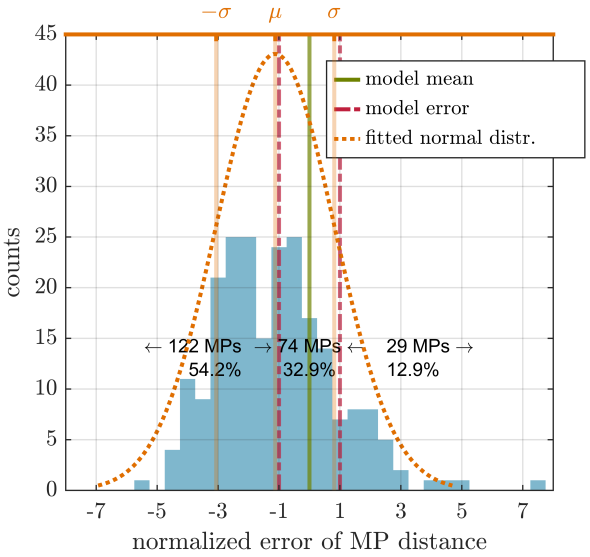

Figure 4. ~~Relative~~ Normalized error of MP ~~position~~distance for innermost crossings. The error ~~width~~ range is indicated by the vertical dashed dotted red line. ~~53.2 %~~ 32.9 % of MP transitions lay within the model error. The mean is at ~~+0.18~~ −1.12, the standard deviation is ~~1.55. The distribution mostly follows a normal distribution. The skewness of 0.30~~ 1.94 and ~~mean indicate a slight tendency of~~ the ~~MP to be found at greater distance to the magnetotail than expected~~skewness is 0.76.

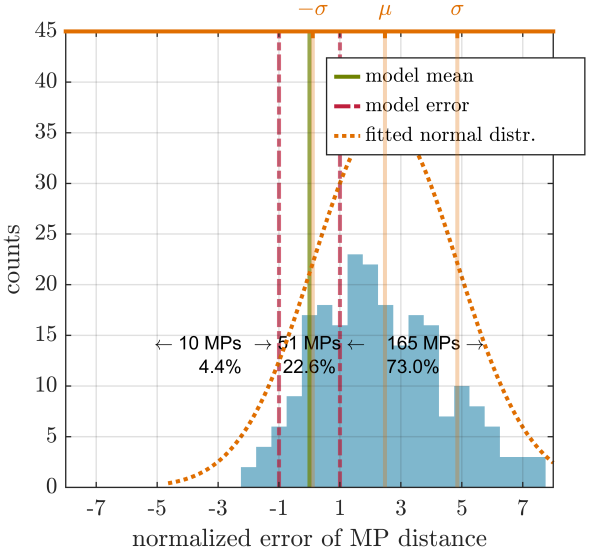

Figure 5. ~~Example for non-existent correlation between the normalized~~ Normalized error of MP distance ~~and~~ for outermost crossings. The error range is indicated by ~~the position~~ vertical dashed dotted red line. 22.6 % of ~~the~~ MP ~~projected onto~~ transitions lay within the ~~x_{GSM}-axis~~model error. The ~~correlation coefficient~~ mean is ~~only $r = 0.37$~~at 2.48, the standard deviation is 2.37 and the skewness is 0.89.

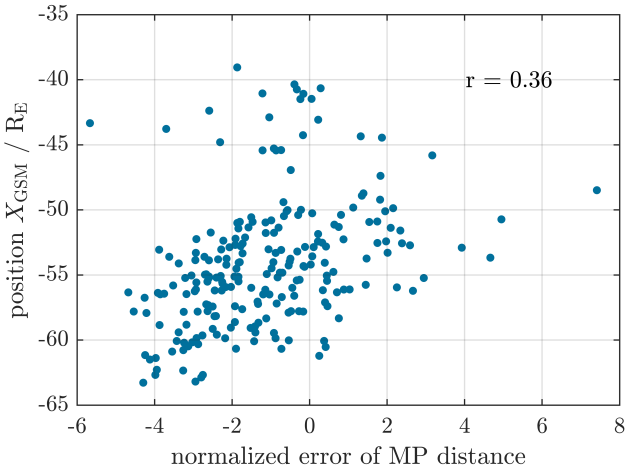

Figure 6. Example for non-existent correlation between the normalized MP distance and the position of the MP crossing projected onto the x_{GSM}-axis for innermost crossings. The correlation coefficient is only $r = 0.36$.

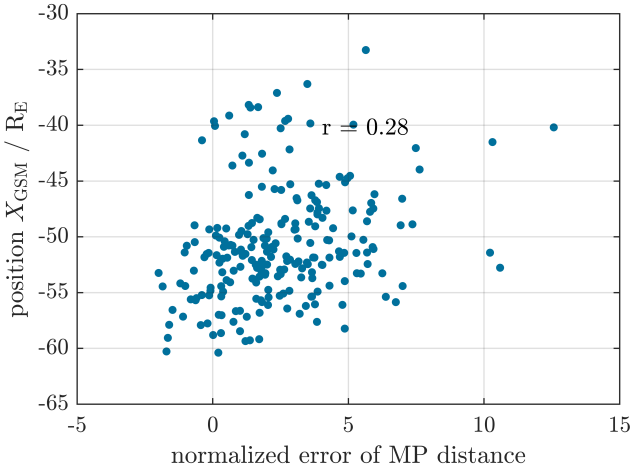

Figure 7. Example for non-existent correlation between the normalized MP distance and the position of the MP crossing projected onto the x_{GSM}-axis for outermost crossings. The correlation coefficient is only $r = 0.28$.

4 Comparison of direction predictions

Besides its radial distance, the direction of the magnetopause normal can also be deduced from the Shue model and compared with the observations at lunar distances. For this purpose model and observed normal directions are projected onto the yz-planes (polar plane) and xy-planes (equatorial), respectively, afterwards the deviation angles α, respectively β, between model and observed normal directions are determined. For deviation angles in the yz-plane (xy-plane) the sign of the angle is defined positive for situations in which the actual direction is pointing towards the positive z (x) direction in relation to the model direction. Figure 8 illustrates this angle convention.

The thus defined deviation angles allow to highlight deviations of the magnetopause's opening angle, in case of the angle laying in xy-plane, which corresponds to the Shue flaring parameter, as well as deviations from the ideal axial symmetry, in case of the angle laying in the yz-plane. For each identified crossing solar wind data is used to calculate the model magnetopause. The expected distribution of angles γ between the model normal direction and the y_{GSM}-axis is shown in Fig. ~~??.~~ 9 for the innermost and Fig. 10 for the outermost crossings. Expected are angles with a mean of ~~5.2 degrees~~ $4.6\,^{\circ}$ ($5.1\,^{\circ}$) for the innermost (outermost) crossing directed sunwards, or positive direction, following our convention. This reinforces the assumption of ~~negligible parallax errors~~a MP almost parallel to the x-axis, see Section 3.

Figures ~~?? and ??~~ 11 and 12 display the deviation angle distributions. ~~For~~

For the innermost crossings we get the following results. The median deviation angles α for the ~~xy_{GSM}~~yz_{GSM}-plane ~~deviations mean values (median values) of $-2.3\,(0.09)$ degrees for~~ are $1.9\,(44.6)\,^{\circ}$ for inbound crossings and ~~$6.0\,(8.73)$ degrees for outbounderossings with standard deviations of 29.2 degrees and 47.2 degrees are found, respectively. Corresponding values for yz_{GSM}~~ $-7.1\,(45.9)\,^{\circ}$ for outbound. Values in parenthesis denote the respective standard deviation. For the angles β, the xy_{GSM}-plane ~~(Figure ?? shows the difference angle between model and data as projected onto the~~ values are $8.0\,(38.3)\,^{\circ}$ for inbound and $5.0\,(42.7)\,^{\circ}$ for outbound. And results for the outermost crossings are as follows. The median deviation angles α for the yz_{GSM}-plane are ~~$4.96\,(4.43)$ degrees respective $-5.32\,(-2.95)$ degrees with standard deviations 33.46 degrees respective 44.66 degrese. The deviation angles exhibit a clear tendency to agglomerate around a vanishing deviation angle~~ $-3.3\,(37.2)\,^{\circ}$ for inbound crossings and $6.1\,(42.7)\,^{\circ}$ for outbound. For the angles β, the xy_{GSM}-plane values are $9.1\,(33.9)\,^{\circ}$ for inbound and $8.3\,(40.2)\,^{\circ}$ for outbound.

Both angles α and β show median values near zero for all cases but come along with high scattering of more than $30\,^{\circ}$. Since we only ~~analysed one~~ observe one single crossing event per spacecraft and month~~as well as the outermost magnetopause traversal, the observed~~ , due to the spacecraft orbit, the high scattering is not surprising. ~~We~~ But, with some caution, we conclude, that ~~predicted normal~~ the predicted directions agree well the actual directions~~, as much as the predicted position does~~.

5 Conclusions

~~Positions~~ The location of the magnetopause at lunar distances ~~show very good agreement with those predicted by the Shue model~~ shows systematic differences to the model prediction. When choosing the innermost crossing of the MP, which is the

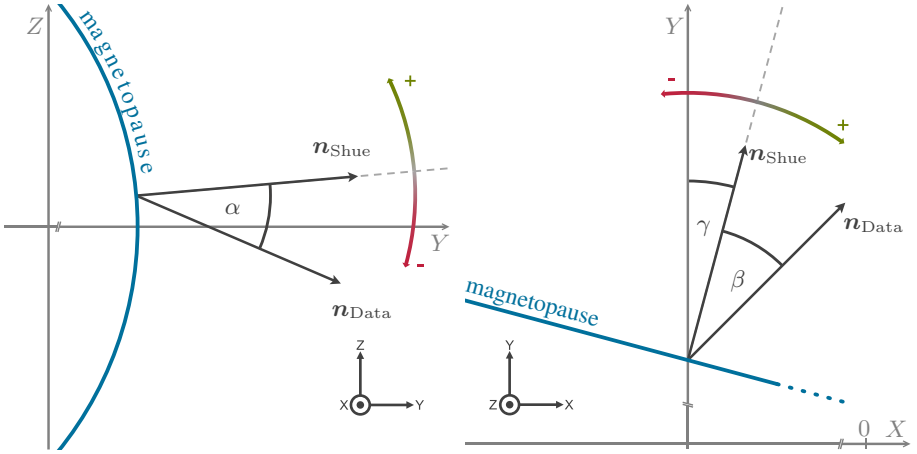

Figure 8. To compare the normal directions of the model and data, angles are measured as deviation from model direction. The angle α (front view, left panel) corresponds to deviation in the rotational symmetry, whereas β (top view, right panel) corresponds to the MP flaring or short term perturbations. The expected opening angle γ of the model is shown in ~~Fig~~Figures 9 and 10.~~??~~

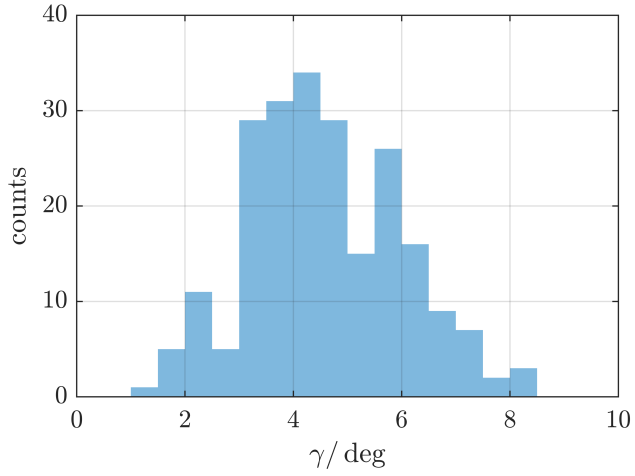

Figure 9. Angle between model MP normal direction of every crossing event and the yz_{GSM}-plane, see angle γ in Fig. 8. Expected are angles with a mean of ~~5.2 degree~~4.6°.

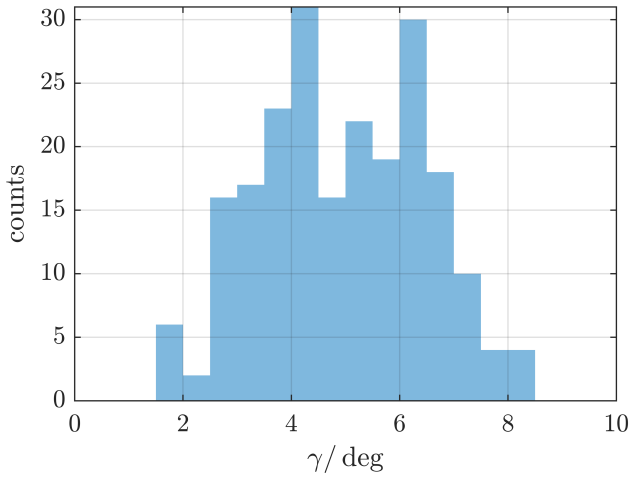

Figure 10. ~~Deviation angle~~ Angle between model ~~and data~~ MP normal direction ~~as projected onto yz_{GSM}-plane (polar plane). The distribution is separated by inbound (red)~~ of every crossing event and ~~outbound (blue) passes. Indicated by~~ the ~~coloured vertical lines are the respective median angles as well as the standard deviations~~yz_{GSM}-plane, see ~~text. The meaning of the~~ angle ~~sign is explained~~ γ in Fig. 8. Expected are angles with a mean of 5.1°.

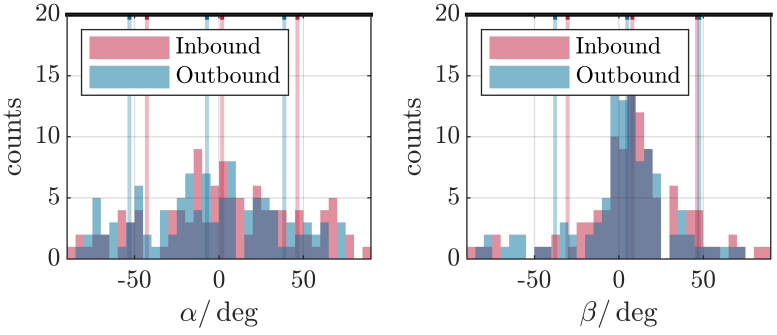

Figure 11. Deviation angle between model and data normal direction as projected onto yz_{GSM}-plane (polar plane), left panel, and as projected onto xy_{GSM}-plane (equatorial plane), right panel, for the innermost crossings. The ~~distribution is~~ distributions are separated by inbound (red) and outbound (blue) passes. Indicated by the coloured vertical lines are the respective median angles as well as the standard deviations, see text. The meaning of the angle sign is explained in Fig. 8.

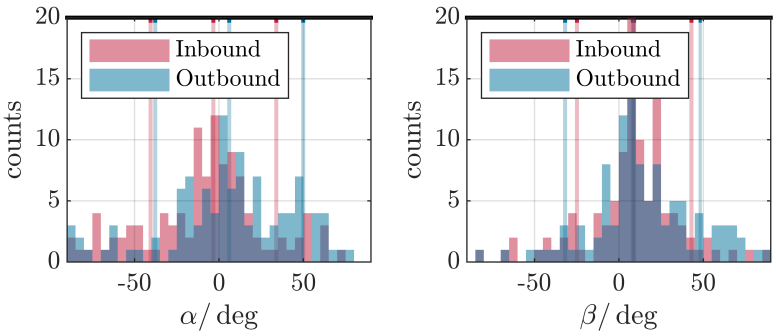

Figure 12. Deviation angle between model and data normal direction as projected onto yz_{GSM}-plane (polar plane), left panel, and as projected onto xy_{GSM}-plane (equatorial plane), right panel, for the outermost crossings. The distributions are separated by inbound (red) and outbound (blue) passes. Indicated by the coloured vertical lines are the respective median angles as well as the standard deviations, see text. The meaning of the angle sign is explained in Fig. 8.

same methodology as in Shue et al. (1997), the location is overestimated. In that case the MP is on average found much closer to the centre of the magnetotail. On the other hand, when choosing the outermost crossing, Shue et al. underestimates the location and the MP is found in much greater distance to the magnetotail centre than expected. ~~The distribution of deviations follows a normal distribution with a normalized standard deviation of about 1.5 in units of the model error width and therefore has very similar statistical properties to the Shue model.~~

~~The magnetopause normal directions~~ Different to this are predictions about the normal direction of the MP. These scatter over a wider range of angles, but show a clear tendency to ~~agglomerate around the~~ conform to the model predicted directions. Since the standard deviation is very large, it is not possible to make a well-founded statement about differences in in- and outbound traversals. Due to the high variability of the magnetopause ~~position~~ location caused by constantly changing solar wind conditions, the scattering in normal direction is as expected, since the SW induces directly changes in the MP standoff distance and indirectly surface waves such as Kelvin-Helmholtz instabilities due to differences in the plasma flow velocity. Essentially, the axial symmetry of the model can be confirmed for lunar distances in the magnetotail and near to the equatorial plane. ~~Also the flaring parameter of the model fits well into our findings despite high scattering.~~

~~On average the Shue model could be validated at lunar distances.~~ We conclude that the ~~model with its consideration of solar wind dynamic pressure and the IMF B_z component most adequately describes the behaviour of magnetopause. Even for the mid-magnetotail these two parameters are the most important drivers for magnetopause movement~~uncertainty in determination of the MP location increases with greater distance to the Earth. This implies that the statistical width f the MP is larger than closer to Earth.

Data availability. THEMIS data and the latest calibration files are publicly available at http://themis.ssl.berkeley.edu/ or via the SPEDAS software.

Competing interests. The authors declare that they have no conflict of interest.

Acknowledgements. We acknowledge use of NASA/GSFC's Space Physics Data Facility's OMNIWeb service, and OMNI data. We acknowledge NASA contract NAS5-02099 and V. Angelopoulos for use of data from the THEMIS Mission - specifically, C. W. Carlson and J. P. McFadden for use of ESA data. This study is financially supported by the German Ministerium für Wirtschaft und Energie and the Deutsches Zentrum für Luft- und Raumfahrt under contract 50 OC 1403.

References

Angelopoulos, V.: The THEMIS Mission, Space Science Reviews, 141, 5–34, https://doi.org/10.1007/s11214-008-9336-1, 2008.

Angelopoulos, V.: The ARTEMIS Mission, Space Science Reviews, 165, 3–25, https://doi.org/10.1007/978-1-4614-9554-3_2, 2010.

Auster, H. U., Glassmeier, K. H., Magnes, W., Aydogar, O., Baumjohann, W., Constantinescu, D., Fischer, D., Fornacon, K. H., Georgescu, E., Harvey, P., Hillenmaier, O., Kroth, R., Ludlam, M., Narita, Y., Nakamura, R., Okrafka, K., Plaschke, F., Richter, I., Schwarzl, H., Stoll, B., Valavanoglou, A., and Wiedemann, M.: The THEMIS Fluxgate Magnetometer, Space Science Reviews, 141, 235–264, https://doi.org/10.1007/s11214-008-9365-9, https://doi.org/10.1007/s11214-008-9365-9, 2008.

Baumjohann, W. and Treumann, R. A.: Basic space plasma physics, Imperial College Press, London, 1996.

Glassmeier, K.-H., Auster, H.-U., Constantinescu, D., Fornaçon, K.-H., Narita, Y., Plaschke, F., Angelopoulos, V., Georgescu, E., Baumjohann, W., Magnes, W., Nakamura, R., Carlson, C. W., Frey, S., McFadden, J. P., Phan, T., Mann, I., Rae, I. J., and Vogt, J.: Magnetospheric quasi-static response to the dynamic magnetosheath: A THEMIS case study, Geophysical Research Letters, 35, https://doi.org/10.1029/2008gl033469, 2008.

Hansen, K. C., Bagdonat, T., Motschmann, U., Alexander, C., Combi, M. R., Cravens, T. E., Gombosi, T. I., Jia, Y.-D., and Robertson, I. P.: The Plasma Environment of Comet 67P/Churyumov-Gerasimenko Throughout the Rosetta Main Mission, Space Science Reviews, 128, 133–166, https://doi.org/10.1007/s11214-006-9142-6, 2007.

Hapgood, M.: Space physics coordinate transformations: A user guide, Planetary and Space Science, 40, 711–717, https://doi.org/10.1016/0032-0633(92)90012-d, 1992.

Lin, R. L., Zhang, X. X., Liu, S. Q., Wang, Y. L., and Gong, J. C.: A three-dimensional asymmetric magnetopause model, Journal of Geophysical Research: Space Physics, 115, https://doi.org/10.1029/2009JA014235, 2010.

McFadden, J. P., Carlson, C. W., Larson, D., Ludlam, M., Abiad, R., Elliott, B., Turin, P., Marckwordt, M., and Angelopoulos, V.: The THEMIS ESA Plasma Instrument and In-flight Calibration, Space Science Reviews, 141, 277–302, https://doi.org/10.1007/s11214-008-9440-2, 2008.

Paschmann, G. and Daly, P. W.: Analysis Methods for Multi-Spacecraft Data, ESA Publications Division, 1998.

Paschmann, G., Baumjohann, W., Sckopke, N., Phan, T. D., and Lühr, H.: Structure of the dayside magnetopause for low magnetic shear, Journal of Geophysical Research: Space Physics, 98, 13 409–13 422, https://doi.org/10.1029/93ja00646, 1993.

Shue, J.-H. and Song, P.: The location and shape of the magnetopause, Planetary and Space Science, 50, 549–558, https://doi.org/10.1016/S0032-0633(02)00034-X, 2002.

Shue, J.-H., Chao, J. K., Fu, H. C., Russell, C. T., Song, P., Khurana, K. K., and Singer, H. J.: A new functional form to study the solar wind control of the magnetopause size and shape, Journal of Geophysical Research: Space Physics, 102, 9497–9511, https://doi.org/10.1029/97ja00196, 1997.

Wang, Y., Sibeck, D. G., Merka, J., Boardsen, S. A., Karimabadi, H., Sipes, T. B., Šafránková, J., Jelínek, K., and Lin, R.: A new three-dimensional magnetopause model with a support vector regression machine and a large database of multiple spacecraft observations, Journal of Geophysical Research: Space Physics, 118, 2173–2184, https://doi.org/10.1002/jgra.50226, 2013.